Electronic Supplementary Material (ESI) for New Journal of Chemistry.

Supporting Information

Ni_xP and Mn_3O_4 dual co-catalysts separately deposited on g-C_3N_4/red phosphorus hybrid photocatalyst for efficient hydrogen evolution

*Qinyi Mao, Dandan Li, Yuming Dong**

International Joint Research Center for Photo-responsive Molecules and Materials, School of Chemical and Material Engineering, Jiangnan University, Wuxi 214122, P. R. China

* Corresponding author, Email: dongym@jiangnan.edu.cn.

Photochemical formation of CNP-Ni-Mn

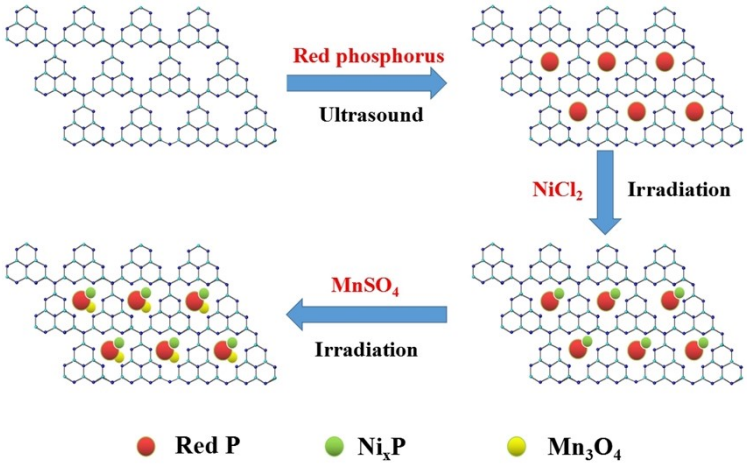

Scheme S1. The proposed photochemical synthesis route of CNP-Ni-Mn.

CNP-Ni-Mn is prepared by a two-step photodeposition process (Scheme S1). The first step is to form reduction co-catalyst Ni_xP on the conduction band by adding $NiCl_2$. During this process, P (0) at the conduction band is reduced to Ni_xP (+δ) by photo-generated electron (eq 2), and P (0) at the valence band is oxidized to PO_x (+δ) (eq 3).

$$CNP + h\nu \rightarrow CNP\,(e^- + h^+) \quad (1)$$

$$P^0 + Ni^{2+} + \delta e^- \rightarrow Ni_xP \quad (2)$$

$$P^0 + \delta h^+ \rightarrow PO_x \quad (3)$$

The second step is to deposit the oxidation co-catalyst Mn_3O_4 at the valence band position. In this process, the product CNP-Ni of the first step was added as a carrier. After photo-excitation generates electrons and holes (eq. 4), hydrogen is producing at the conduction band position due to the presence of the reduction co-catalyst (eq. 5), and the generated hydrogen gas has been measured by gas chromatography. At the valence band position, Mn^{2+} is oxidized by photo-generated holes to form oxidation co-catalyst Mn_3O_4 (eq. 6).

$$CNP\text{-}Ni + h\nu \rightarrow CNP\text{-}Ni\,(e^- + h^+) \quad (4)$$

$$2H^+ + 2e^- \rightarrow H_2 \quad (5)$$

$$3Mn^{2+} + 6h^+ + 4H_2O \rightarrow Mn_3O_4 + 6H^+ \quad (6)$$

Table S1. Conditions of control experiments.

	CNP /mg	$NiCl_2$ (0.1M) /mL	$MnSO_4$ (0.1M) /mL	H_2O /mL	Irradiation time /min	Heating time (50℃) /min	Stirring time /min
A	30	-	1	9	50	-	-
B	30	1	-	9	50	-	-
C	30	1	1	8	50	-	-
D	30	-	1	9	50	-	-
	30(CNP-Mn)	1	-	9	50	-	-
E	30	1	-	9	50	-	-
	30(CNP-Ni)	-	1	9	50	-	-
F	30	1	-	9	-	50	-
	30(CNP-Ni)	-	1	9	-	50	-
G	30	1	-	9	-	-	50
	30(CNP-Ni)	-	1	9	-	-	50
H	30(P + CN)	1	-	9	50	-	-
	30(P/CN-Ni)	-	1	9	50	-	-

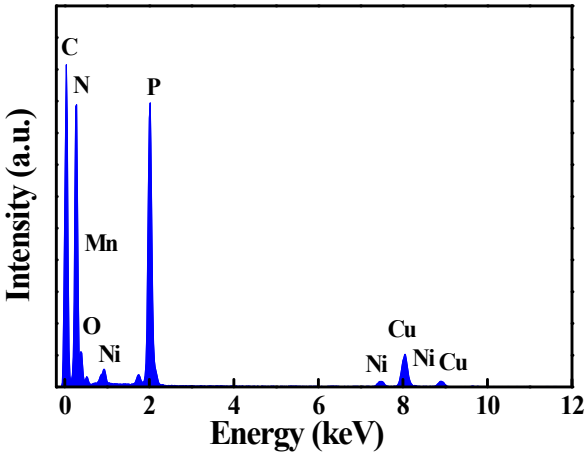

Fig. S1. TEM-EDX of CNP-Ni-Mn.

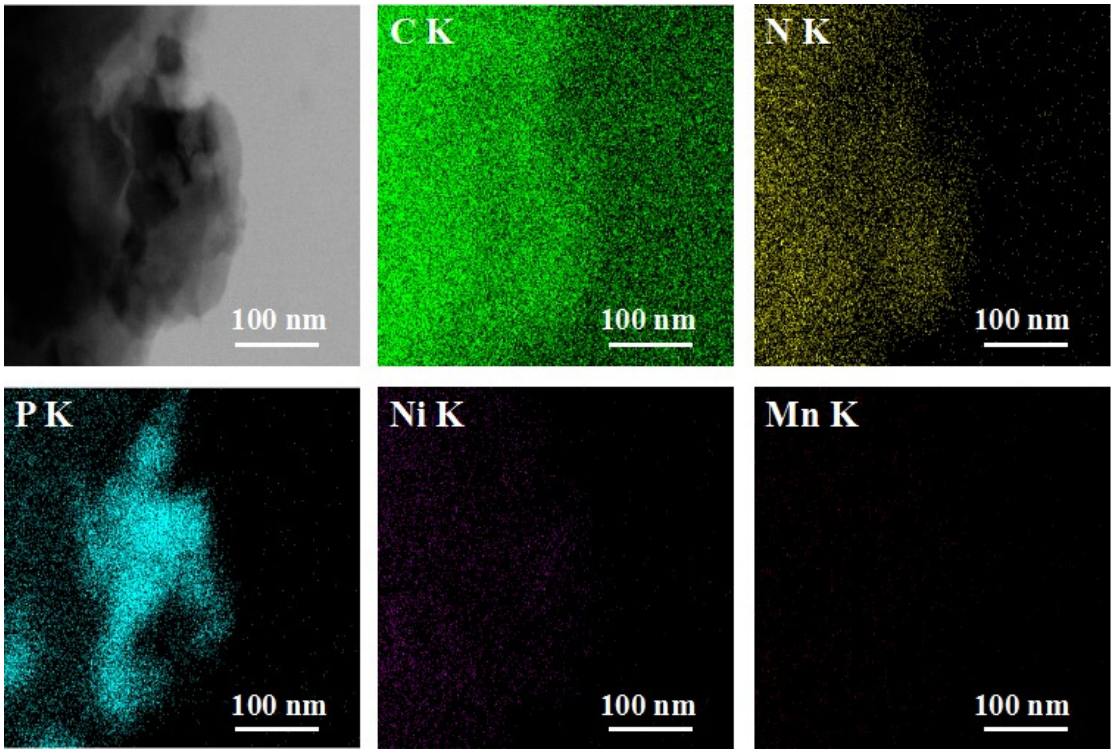

Fig. S2. EDX-Mapping images of C, N, P, Ni and Mn elements in CNP-Ni-Mn.

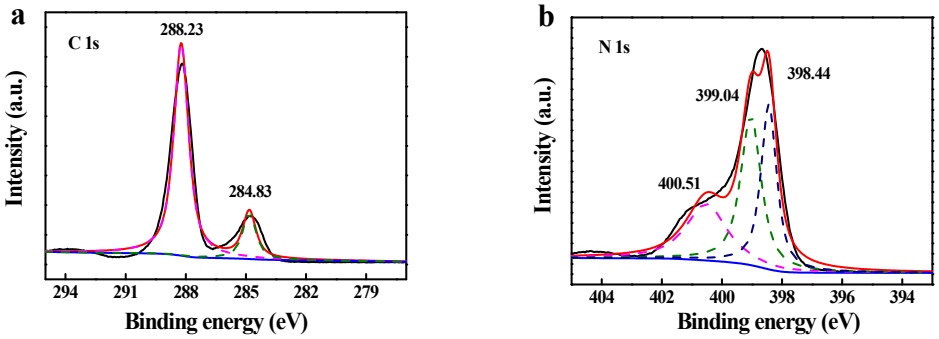

Fig. S3. The high-resolution XPS spectra of C 1s (a) and N 1s (b) in pure g-C_3N_4.

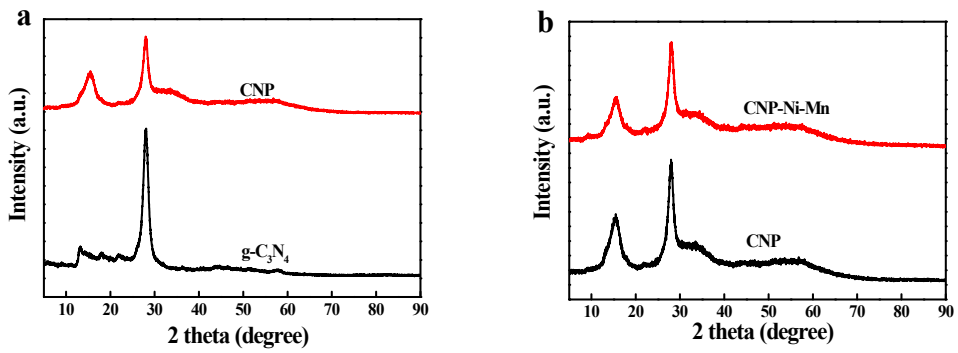

Fig. S4. The XRD patterns of g-C_3N_4 and CNP (a), CNP and CNP-Ni-Mn (b).

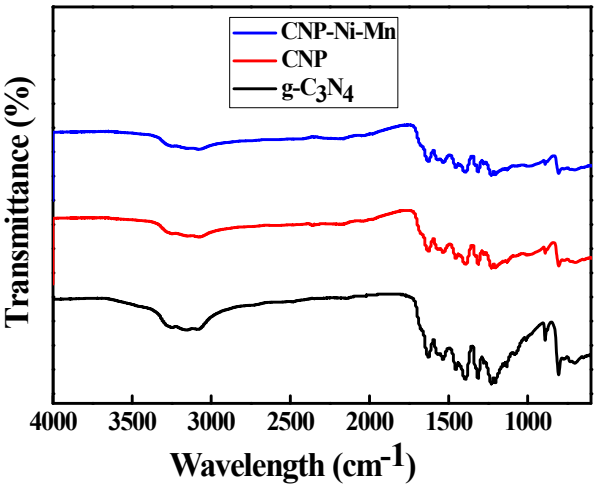

Fig. S5. FT-IR spectroscopy of g-C_3N_4, CNP and CNP-Ni-Mn.

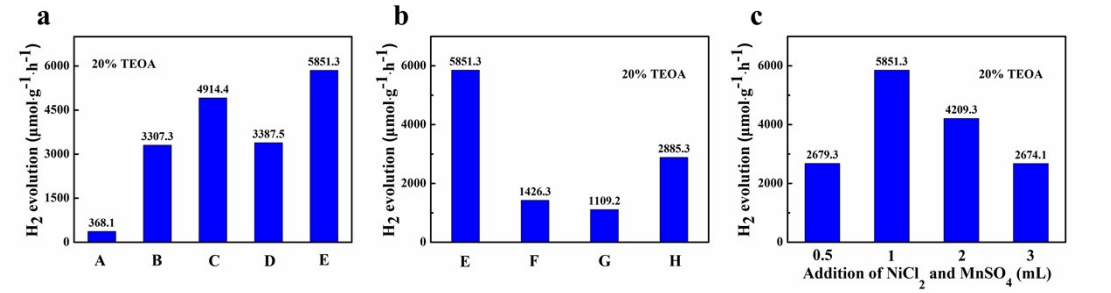

Fig. S6. (a) Photocatalytic hydrogen production activity of catalyst A-E in 20 vol% TEOA solution in Table 1. (b) Comparison of irradiation (E), heating (F), stirring (G) and red phosphorus (H) in 20 vol% TEOA solution. (d) Photocatalytic hydrogen production activity of different addition amount of $NiCl_2$ and $MnSO_4$ (1:1) in 20 vol% TEOA solution.

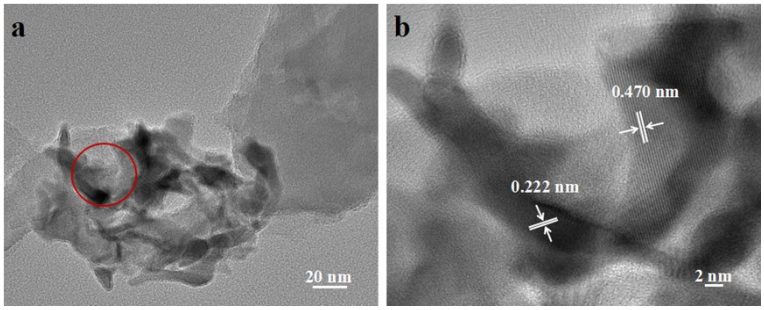

Fig. S7. TEM (a) and HR – TEM (b) of CNP-Ni-Mn after photocatalysis. The measured lattice fringes of 0.222 nm and 0.470 nm correspond to the (111) crystal face Ni_2P and the (200) crystal face of Mn_2O_3.

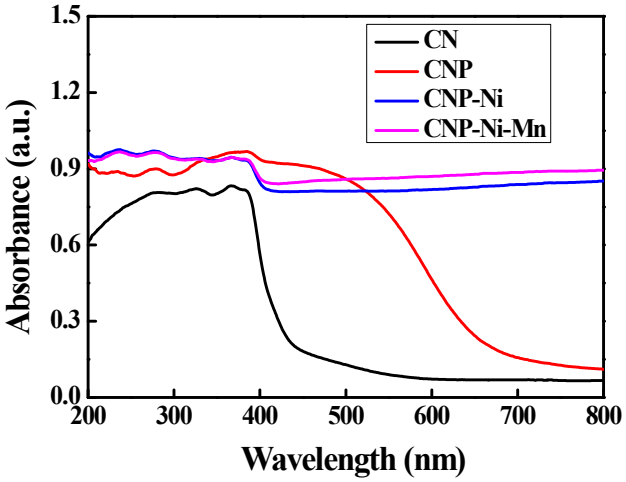

Fig. S8. UV-vis diffuse reflectance spectroscopy of pure g-C_3N_4, CNP, CNP-Ni and CNP-Ni-Mn.

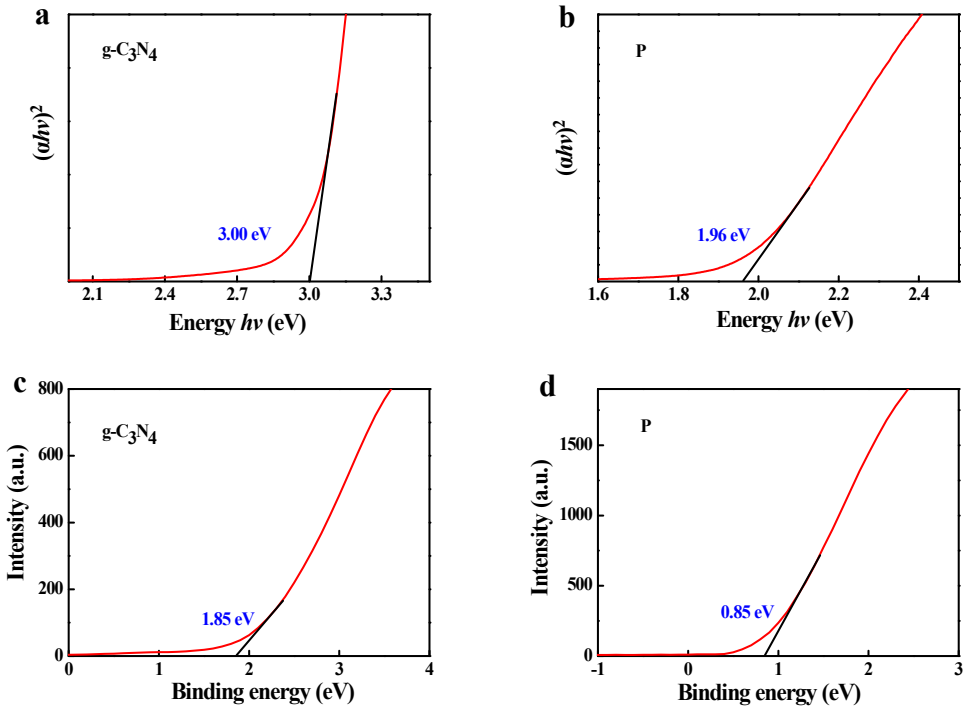

Fig. S9. Tauc plots of g-C_3N_4 (a) and red P (b). XPS spectra of g-C_3N_4 (c) and red P (d) for valence band offset determination.

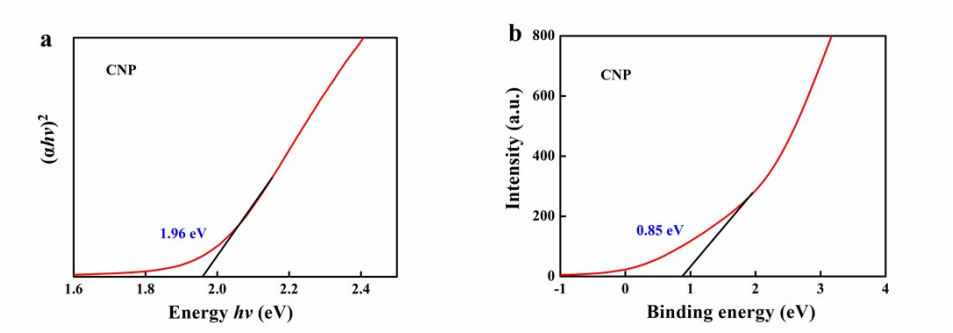

Fig. S10. (a) Tauc plots of CNP. (b) XPS spectra of CNP for valence band offset determination.

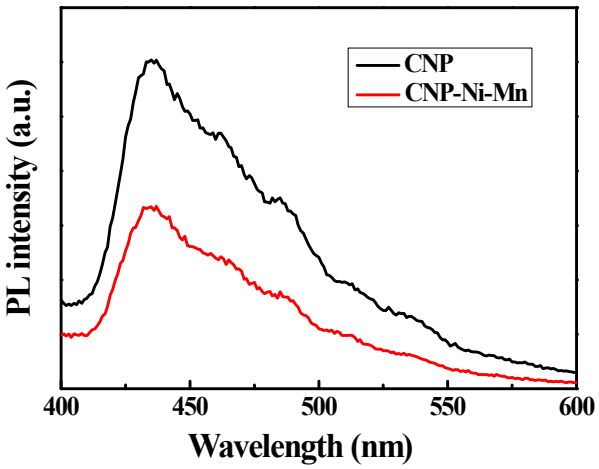

Fig. S11. PL spectra of CNP and CNP-Ni-Mn under the excitation wavelength of 375 nm.

Table S2. The co-catalysts for photocatalytic hydrogen evolution reaction.

Photocatalyst	Co-catalysts	Light source	Sacrificial agent	Activity (μmol h^{-1} g^{-1})	Stability at least (h)	Ref. (year)
g–C_3N_4/WO_3	$Ni(OH)_x$	λ > 400 nm (Xe)	TEOA	576	12	[1] (2017)
g–C_3N_4	Co	AM 1.5 (Xe)	TEOA	2296	48	[2] (2018)
g–C_3N_4	MoS_2	λ ≥ 400 nm (Xe)	Lactic acid	660	9	[3] (2018)
N–TiO_2/g–C_3N_4	Ni_xP	780 > λ > 350 nm (Xe)	TEOA	5438	10	[4] (2018)
TiO_2	CuO_x	AM 1.5G (Xe)	Methanol	407	—	[5] (2018)
$CaIn_2S_4$	MnO_x	750 nm ≥ λ ≥ 420 nm (Xe)	Na_2S + Na_2SO_3	5520	—	[6] (2019)
g–C_3N_4	NiS, CoS_x, CuS_x	420 nm (LED)	TEOA	244	7.5	[7] (2021)
g-C_3N_4	Ni–Ag	λ ≥ 420 nm (Xe)	Methanol	2137.5	16	[8] (2022)
g-C_3N_4/red P	Ni_xP-Mn_3O_4	AM 1.5 (Xe)	TEOA	5851.3	8	This work

1. K. He, J. Xie, X. Luo, J. Wen, S. Ma, X. Li, Y. Fang and X. Zhang, *Chinese J. Catal.*, 2017, **38**, 240-252.
2. W. Chen, Y. Wang, M. Liu, L. Gao, L. Mao, Z. Fan and W. Shangguan, *Appl. Surf. Sci.*, 2018, **444**, 485-490.
3. X. Shi, M. Fujitsuka, S. Kim and T. Majima, *Small*, 2018, **14**, e1703277.
4. M. Wu, J. Zhang, C. Liu, Y. Gong, R. Wang, B. He and H. Wang, *ChemCatChem*, 2018, **10**, 3069-3077.
5. P. A. Bharad, A. V. Nikam, F. Thomas and C. S. Gopinath, *ChemistrySelect*, 2018, **3**, 12022-12030.
6. J. Ding, X. Li, L. Chen, X. Zhang, H. Yin and X. Tian, *ACS Appl. Mater. Interfaces*, 2019, **11**, 835-845.
7. M. Wang, J. Cheng, X. Wang, X. Hong, J. Fan and H. Yu, *Chinese J. Catal.*, 2021, **42**, 37-45.
8. F. Sarwar, M. Tahir and H. Alias, *Mater. Sci. Semicond. Process.*, 2022, **137**.